



## Research paper

# Design, modeling, and expression of erythropoietin cysteine analogs in *Pichia pastoris*: Improvement of mean residence times and in vivo activities through cysteine-specific PEGylation

Ahmad Maleki<sup>a,b</sup>, Armin Madadkar-Sobhani<sup>c,d</sup>, Farzin Roohvand<sup>e,\*</sup>, Abdolhossein R. Najafabadi<sup>a</sup>, Abbas Shafiee<sup>a</sup>, Hossein Khanahmad<sup>b</sup>, Reza A. Cohan<sup>b</sup>, Nabiallah Namvar<sup>b</sup>, Hosnieh Tajerzadeh<sup>a,\*</sup>

<sup>a</sup> Department of Pharmaceutics, The Tehran University of Medical Science, Tehran, Iran

<sup>b</sup> Pasteur Institute of Iran, Research and Production Complex, Karadj, Iran

<sup>c</sup> Department of Bioinformatics, The University of Tehran, Tehran, Iran

<sup>d</sup> Department of Life Sciences, The Barcelona Supercomputing Center, Barcelona, Spain

<sup>e</sup> Department of Hepatitis and AIDS, Pasteur Institute of Iran, Tehran, Iran

## ARTICLE INFO

## Article history:

Received 27 June 2011

Accepted in revised form 24 October 2011

Available online 31 October 2011

## Keywords:

Erythropoietin cysteine analogs

*Pichia pastoris*

Cysteine-specific PEGylation

Pharmacokinetics

Bioactivity

## ABSTRACT

In this study, the low-cost production of recombinant human erythropoietin cysteine analogs (Cys-rhEPOs) from *Pichia pastoris* and the potential to increase their serum residency and in vivo activity through cysteine-specific PEGylation were investigated. Three-dimensional structures of several Cys-rhEPOs were generated using homology modeling, and three stable Cys-rhEPOs were selected on the basis of model stability in molecular dynamics simulation and surface accessibility of the inserted cysteine. cDNAs encoding Cys-rhEPOs were constructed by site-directed mutagenesis and expressed as secreted proteins in flask cultures of *P. pastoris*. The selection of highly expressing clones and the optimization of certain culture parameters resulted in protein expression levels of 100–170 mg/l. Purified Cys-rhEPOs were cysteine-specifically PEGylated using 20 kDa and 30 kDa mPEG-maleimides (methoxy polyethylene glycol-maleimides). The E89CEPO analog with the highest (96.6%) cysteine accessibility was conjugated to PEG-polymers with the largest yields (about 80%). In comparison with rhEPO, 30 kDa PEG-E89CEPO demonstrated a significant (approximately 30%) increase in the mean residence time. Whereas the in vitro activities of 30 kDa PEG-E89CEPO were comparable to those of rhEPO, the in vivo activity of this conjugate was more prolonged compared to rhEPO (12 days vs. 7 days). Our results demonstrate that the site-specific PEGylation of *Pichia*-expressed EPO analogs may be considered as a promising approach for generating cost-effective and long-acting erythropoiesis-stimulating agents.

© 2011 Elsevier B.V. All rights reserved.

## 1. Introduction

Erythropoietin (EPO) is a glycoprotein hormone with an average molecular weight (MW) of 30 kDa, and it functions as a

hematopoietic growth factor [1]. This therapeutic protein is used in the treatment of several major anemic disorders, and currently, its high clinical demand has been fulfilled using recombinant DNA technology and through the expression of the human EPO gene in Chinese Hamster Ovary (CHO) cells [2]. The introduction of recombinant human EPO (rhEPO) into clinical practice has prompted many researchers to investigate numerous approaches to develop more economical ways to produce erythropoiesis-stimulating agents (ESAs) that have prolonged in vivo activities and expanded dosing intervals and thus offering more advantages to patients.

To address the issue of producing of rhEPO in a more cost-effective manner, different prokaryotic and eukaryotic expression systems, such as *Escherichia coli* [3], *Bacillus brevis* [4], *Saccharomyces cerevisiae* [5], and *Pichia pastoris* [6,7] have been investigated. Among these common expression systems, the methylotrophic yeast "*P. pastoris*" is well known for its high-yield and low-cost

**Abbreviations:** rhEPO, recombinant human erythropoietin; ESA, erythropoiesis-stimulating agents; PEG, polyethylene glycol; Cys-rhEPO, cysteine analogs of rhEPO; DAB, 3,3'-diaminobenzidine; MTT, 3-[4,5-dimethylthiazol-2-yl]-2,5-diphenyl tetrazolium bromide; PCR, polymerase chain reaction; PVDF, polyvinylidene fluoride;  $\alpha$ MEM, alpha-modified minimum essential medium; FBS, fetal bovine serum; TCEP, Tris (2-carboxyethyl) phosphine-HCl; GM-CSF, granulocyte-macrophage colony-stimulating factor.

\* Corresponding authors. Department of Hepatitis and AIDS, Pasteur Institute of Iran, 1316943551 Tehran, Iran (F. Roohvand). Department of Pharmaceutics, The Tehran University of Medical Science, Faculty of Pharmacy, 1417653761 Tehran, Iran (H. Tajerzadeh). Tel.: +98 21 66959053; fax: +98 21 66461178.

E-mail addresses: [rfarzin@pasteur.ac.ir](mailto:rfarzin@pasteur.ac.ir) (F. Roohvand), [tajerzadeh@tums.ac.ir](mailto:tajerzadeh@tums.ac.ir) (H. Tajerzadeh).

production of many therapeutic proteins [8]. In fact, *P. pastoris* offers the benefits of both prokaryotic and eukaryotic expression systems and provides the potential for simple and economical production of heterologous proteins that are secreted in large quantities at the same time, and it is able to execute post-translational modifications, such as proper folding, correct disulfide bond formation, and proteolytic processing [9]. However, *P. pastoris* is not capable of adding terminal sialic acid residues during the glycosylation of recombinant proteins. It has been shown that the terminal sialylation in these sugar chains plays an essential role in the in vivo activity of EPO [10], and accordingly, *Pichia*-expressed EPO exhibits no in vivo activity in rabbit [7]. To this end, Hamilton et al. [11] engineered *P. pastoris* to express complex terminally sialylated glycoproteins and utilized this strain to produce *Pichia*-expressed rat-EPO that had retained its in vivo bioactivity. The modification of proteins with polyethylene glycol (PEG) is an alternative and well-established technique for improving biological and pharmacokinetic characteristics of therapeutic proteins [12]. Emerging data suggest that this process, known as PEGylation, may parallel the critical role native glycosylation plays in conferring in vivo activity on non-sialylated EPO proteins [3,7,13].

Recently, we reported the N-terminal PEGylation of *Pichia*-expressed rhEPO (PPEPO) using reductive alkylation of the protein with a 20 kDa mPEG-propionaldehyde under low pH conditions [7]. The mean residence time (MRT) and in vivo activity of 20 kDa PEG-PPEPO were comparable with those of rhEPO. The results encouraged us to investigate various aspects of PEGylation to further improve the bioactivity and pharmacokinetic properties of *Pichia*-expressed rhEPO.

In this study, we describe the flask-expression of three engineered cysteine analogs of rhEPO (Cys-rhEPO) in *P. pastoris*. For each Cys-rhEPO, a single amino acid in a non-functional region of the protein was selected and replaced with a free cysteine residue, which allowed the protein to conjugate with Cys-specific PEGylating reagents (i.e., mPEG-maleimide) through the sulfhydryl group of the engineered cysteine [14]. Rational selection of non-functional amino acid candidates for replacement with a cysteine residue was carried out using computational modeling. To this end, three-dimensional (3D) structures of a number of Cys-rhEPOs were generated using homology modeling and molecular dynamics (MD) simulations. During MD simulation, three stable Cys-rhEPOs (A1CEPO, E89CEPO, and R162CEPO) were selected based on the surface accessibility of the inserted cysteine in modeled analogs. Cysteine-targeted PEGylation of selected Cys-rhEPOs was carried out using 20 kDa and 30 kDa mPEG-maleimides under reducing conditions. The in vitro activities of the PEG-Cys-rhEPO conjugates were measured using an EPO-dependent cell proliferation assay. The in vivo activities and pharmacokinetic profiles of the PEG-E89CEPO conjugate were compared with those of CHO-derived rhEPOs. Our results demonstrate that site-specific PEGylation of *Pichia*-derived EPO proteins is a promising approach for the development of a new group of ESAs that can be produced at a lower cost and with superior activities compared with the erythropoietic agents that are presently available.

## 2. Materials and methods

### 2.1. Construction of vectors for the expression and secretion of Cys-rhEPOs in *P. pastoris*

Plasmid p57EPO, harboring the human EPO cDNA (NCBI accession No. NM\_000799) in tandem with DNA encoding six histidine amino acids at the C-terminal (C-6xHis-tag), was constructed by Bio Basic Inc., Canada. Using p57EPO as a template, cDNAs

encoding the Cys-rhEPOs were constructed by site-directed PCR-based mutagenesis [15], exploiting different combinations of custom-designed primer pairs (TAG Copenhagen, Denmark). PCR-amplified fragments were gel-purified and were ligated separately into the pPICZαA vector (Invitrogen, USA) that was previously digested with *Xho*I and *Xba*I restriction enzymes (Fermentas, Canada). The products of each ligation reaction were used to transform *E. coli* TOP10 (Invitrogen) competent cells. The presence and accuracy of the inserted genes into the expression cassette in the final recombinant constructs was confirmed by PCR, restriction analyses, and DNA sequencing using the 5'AOX1 and 3'AOX1 primer pairs (Invitrogen).

### 2.2. Transformation of *P. pastoris* and selection of high expressing clones

The recombinant plasmids were purified, linearized with *Sac*I (Fermentas), and electroporated separately into the yeast *P. pastoris* wild-type host strain X-33 according to the manufacturer's instructions (Easy Select *Pichia* Expression manual, Invitrogen). Electroporation was performed in 0.2 cm cuvettes at 1.5 kV using a Bio-Rad Gene Pulser. Mut<sup>+</sup> (methanol utilization positive) transformants were selected in a primary screen using 100 µg Zeocin/ml and were reselected on YPD agar plates comprised of 1% (w/v) yeast extract, 2% (w/v) peptone, 2% (w/v) dextrose and 2% (w/v) agar supplemented with 1 M sorbitol and 2.0 mg Zeocin/ml. Finally, for each EPO construct, 10 Zeocin-resistant transformants were cultured and induced with methanol in 50 ml conical tubes for the selection of highly expressing clones. For each Cys-rhEPO, the clone with the highest expression level of recombinant protein was selected using ELISA and Western blot analysis.

### 2.3. Expression and purification of Cys-rhEPOs

For each Cys-rhEPO, a single colony was inoculated into 5 ml of YPD medium and grown overnight at 30 °C (200 rpm). The seed culture was inoculated into 100 ml BMGY medium [1% (w/v) yeast extract, 2% (w/v) peptone, 1.34% (w/v) YNB,  $4 \times 10^{-5}$ % (w/v) biotin, 1% (v/v) glycerol, and 0.1 M potassium phosphate, pH 6.0], and growth was allowed to proceed at 30 °C (200 rpm) for 16–18 h. Cells were harvested by centrifugation (3000 g for 4 min at 25 °C), and the pellet was resuspended in 200 ml BMMY medium [1% (w/v) yeast extract, 2% (w/v) peptone, 1.34% (w/v) YNB,  $4 \times 10^{-5}$ % (w/v) biotin, 0.5% (v/v) methanol, and 0.1 M potassium phosphate, pH 6.0] in a 2 liter baffled Erlenmeyer flask (OD<sub>600</sub> ~ 1–2) and incubated at 28–30 °C (250 rpm) for 72 h. Induction was achieved by the addition of 1% (v/v) methanol into the fed batch mode every 24 h. During the induction period, phosphoric acid was used to maintain the culture medium at pH 6 ± 0.5. A final concentration of 2 mM cysteine was added to the supernatants at the end of induction period and before protein harvesting. The proteins were harvested by centrifuging the medium at 10,000 g for 10 min (4 °C), and the supernatant was concentrated 10-fold using a Pellicon XL50 ultrafiltration cassette (Millipore, USA) equipped with an Ultracel membrane (MW cutoff of 10 kDa). To purify the recombinant proteins, an AKTA purifier protein purification system (GE Healthcare Inc., Sweden) was used. Each concentrated sample was loaded at a rate of 0.8 ml/min onto a Ni<sup>2+</sup>-charged affinity chromatography column (5 ml His Trap HP column, GE Healthcare Inc.) that was pre-equilibrated with 20 mM sodium phosphate buffer containing 0.5 M sodium chloride, pH 7. The column was washed with 100 ml of washing buffer (equilibration buffer plus 80 mM imidazole), and bound proteins were subsequently eluted with elution buffer (equilibration buffer plus 250 mM imidazole). Purification was carried out by Size Exclusion (SE) chromatography (HiLoad

Superdex 75 prep grade, GE Healthcare Inc.) using a 50 mM sodium phosphate solution containing 150 mM sodium chloride, pH 7, as an equilibration and elution buffer. Purified Cys-rhEPOs were stored at  $-80^{\circ}\text{C}$  until further analysis.

#### 2.4. Cysteine-specific PEGylation of Cys-rhEPO proteins

A 1 mg/ml solution of Cys-rhEPO or PPEPO [7] in 50 mM Tris buffer, pH 8.0 was added to a 30-fold molar excess of TCEP [Tris(2-carboxyethyl)phosphine-HCl] (Sigma–Aldrich) and a 30-fold molar excess of 20 kDa and/or 30 kDa mPEG-maleimide (SunBio Inc, South Korea), and the reaction was incubated at  $25^{\circ}\text{C}$  under nitrogen. After 3 h, each PEGylation reaction was diluted 10-fold with 20 mM Tris buffer, pH 8.0. The solution was loaded at a rate of 1 ml/min onto a 5 ml HiTrap Q-Sepharose column (GE Healthcare Inc.) that was previously equilibrated with 20 mM Tris buffer, pH 8.0. The column was washed with 40 CV (column volume) of equilibration buffer to wash away any unbound PEGs. The bound PEGylated proteins were then resolved by elution with a 0–300 mM NaCl gradient in equilibration buffer. The eluted PEG-Cys-rhEPO fractions were passed through a Superdex 200 10/30 column (GE Healthcare Inc.) that was pre-equilibrated in 50 mM sodium phosphate buffer, pH 7.0 containing 150 mM NaCl. The PEG conjugates were eluted using the equilibration buffer and were sterile filtered and stored at  $-80^{\circ}\text{C}$ .

SE-HPLC (using a Shodex column PROTEIN KW-802.5, Japan) was employed to analyze the purity and yield of the PEG-Cys-rhEPO conjugates. A solution of 50 mM sodium phosphate buffer, pH 7 containing 150 mM NaCl was used as an equilibration and elution buffer.

#### 2.5. UT-7 cell proliferation bioassay

UT-7 cell lines were purchased from DSMZ (German Collection of Microorganisms and Cell Cultures, Germany) and maintained in  $\alpha$ MEM medium supplemented with 10% (w/v) FBS, 40 mg/ml gentamycin, 2 mM glutamine, and 5 ng/ml GM-CSF (Sigma–Aldrich). For bioassays, the cells were washed twice by centrifugation in the assay medium (the growth medium lacking GM-CSF). Cell number and trypan blue cell viability were determined, and the cells were resuspended in the assay medium to a final concentration of  $1 \times 10^5$  cells/ml. Subsequently, 50  $\mu\text{l}$  of the cell suspension was dispensed into each well of a 96-well tissue culture plate (with the exception of the blank controls). Serial 2-fold dilutions of Cys-rhEPOs or PEG-Cys-rhEPO conjugates were prepared in the assay medium. Each diluted sample (50  $\mu\text{l}$ ) was added to test wells in triplicate, and plates were incubated for 3 days at  $37^{\circ}\text{C}$  in a humidified 5%  $\text{CO}_2$  incubator. Cell growth was evaluated using the colorimetric MTT assay [16]. For each test, a blank containing the complete medium without cells was included to measure the background absorbance.

#### 2.6. Pharmacokinetic studies

All in vivo protocols and animal experiments received prior approval from the ethical committee of the Pasteur Institute of Iran. Male New Zealand White rabbits, weighing 1.3–1.5 kg, were obtained from the Pasteur Institute of Iran. Four groups, each consisting of three animals, were intravenously injected with rhEPO (R&D Systems Inc., USA), E89CEPO, 20 kDa PEG–E89CEPO or 30 kDa PEG–E89CEPO at a dose of 15  $\mu\text{g/kg}$ . Blood samples (1 ml) were drawn via the marginal ear vein prior to the initial injection and post-injection at selected time points for up to 72 h. Serum samples were isolated, stored at  $-70^{\circ}\text{C}$  and, following appropriate dilution, analyzed using human EPO ELISA kits (Roche Diagnostics GmbH, Germany) to determine the circulating

concentrations of E89CEPO and the PEG conjugates. The measuring range of ELISA was from 2.8 to 200 mIU EPO/ml with a limit of detection (LOD) of 0.24 mIU/ml. Compartmental pharmacokinetic studies were conducted to analyze the concentration versus time data up to 72 h. The terminal half-life was determined from linear regression of the last three serum concentration–time points (i.e., 24–72 h), except for the E89CEPO terminal half-life, which was derived from concentration–time points 1–24 h post-injection. The area under the plasma level–time curve (AUC) and the area under the moment curve (AUMC) were estimated using the linear trapezoidal method with extrapolation to infinity.

#### 2.7. In vivo efficacy assay

The hematopoietic activity of E89CEPO and the PEG–E89CEPO conjugates was evaluated and compared with that of rhEPO (R&D Systems) using the normocythemic mice assay. Groups of six normal, 8-week old, healthy B6D2F1 mice were weighed, and each received a single subcutaneous injection of samples at a dose of 10  $\mu\text{g}$  protein/kg. Blood samples were drawn via the tail vein at 0, 2, 4, 7, 10, and 14 days after injection. EDTA-treated whole blood from each sample (3  $\mu\text{l}$ ) was added to tubes containing 2 ml of thiazole orange (0.1  $\mu\text{g/ml}$ ) in Dulbecco's Phosphate-Buffered Saline (Invitrogen), mixed thoroughly and incubated for 30 min in the dark at room temperature. Absolute RET counts and the percentage of reticulocyte counts (RET%) in red blood cells were then determined microfluorometrically using a Beckman Coulter flow cytometer.

#### 2.8. In silico studies

Three-dimensional structures of Cys-rhEPOs were generated by homology modeling using MODELLER [17] version 9.5 and the crystal structure of EPO (PDB code: 1EER, chain A, 1.9 Å) as a template. For each Cys-rhEPO or native EPO, 10,000 molecules were generated, and the one corresponding to the lowest value of probability density function was selected. The quality of the models was checked using the Discrete Optimized Protein Energy (DOPE) score profile and a Ramachandran plot. The stability of modeled Cys-rhEPOs was examined by MD simulation with explicit waters using the GROMACS 3.3 package and Gromos 96 force field [18]. MD simulations were carried out at constant temperature (300 K) and pressure (1 bar) for 5–15 ns. After calculating the average structures corresponding to the last 500–2000 ps of MD simulations, modeled Cys-rhEPO analogs with a root mean square deviation (RMSD) of less than 4 Å from an initial structure were chosen for further analysis. All-atom RMSDs between native EPO and selected Cys-rhEPOs were calculated using Qmol software [19]. The surface area accessibility of engineered cysteine residues (cysteine-SAA) in modeled Cys-rhEPOs was computed with the GETAREA server [20].

#### 2.9. EPO protein analysis

The concentrations of EPO proteins in the appropriately diluted supernatants were quantified using a human EPO ELISA kit (Roche Diagnostics GmbH) according to the manufacturer's instructions. Concentrations of total purified EPO proteins and PEG-Cys-rhEPO conjugates were measured using the Bradford method [21]. Protein samples were analyzed using the standard Laemmli SDS–PAGE method [22] on a 12.5% separating gel and developed with silver staining methods. Western analysis was performed by electroblotting proteins from the SDS–PAGE gel to Whatman nitrocellulose membranes (Schleicher & Schuell, UK). Proteins were detected using the monoclonal anti-rhEPO antibody (R&D Systems) and/or the monoclonal anti-6xHis antibody (Invitrogen) and the

horseradish peroxidase-conjugated goat anti-mouse IgG (Promega Co., USA) secondary antibody. The bands were developed using the DAB chromogenic substrate (Sigma–Aldrich). Cell concentrations were measured with a Perkin–Elmer UV/VIS spectrophotometer at an absorbance of 600 nm using a calibration curve. Statistical analyses of the data were performed using a Student's *t*-test and a one-way multivariate ANOVA to calculate the level of significance (*p*-value). Values of *p* < 0.05 were considered statistically significant.

### 3. Results and discussion

#### 3.1. Construction of vectors and selection of high expressing clones

For the secreted expression of Cys-rhEPOs in *P. pastoris*, the plasmid PICZ $\alpha$ A, which contains the  $\alpha$ -factor secretion signal sequence, was used to construct three recombinant shuttle-vectors (pPICZ $\alpha$ A::A1CEPO, pPICZ $\alpha$ A::E89CEPO, and pPICZ $\alpha$ A::R162CEPO) (Fig. 1). The *Xho*I and *Xba*I restriction sites were inserted into the forward and backward primers, respectively, to allow the direct cloning of amplicons in pPICZ $\alpha$ A in frame with alcohol oxidase (*AOX1*) transcription cassette and downstream of the  $\alpha$ -factor. Employing the *Xho*I site allowed the Cys-rhEPOs genes to be inserted immediately after the Kex2 signal cleavage site. In addition, the presence of the C-6xHis-tag codons before the stop codons in p57EPO (original template) excluded further use of the pPICZ $\alpha$ A-coding 6xHis-tag. This cloning strategy resulted in the secreted expression of the Cys-rhEPOs consisting of 166 amino acids plus the C-6xHis-tag without any vector derived amino acids in protein's C- or N-terminals. The presence and authenticity of the Cys-rhEPOs genes in the recombinant constructs were confirmed using PCR (using appropriate primers), restriction analyses, and DNA sequencing reactions (data not shown).

Due to the advantages of electroporation, e.g., a high frequency of transformation and the possibility of multi-copy insertions (*Pichia* Expression manual, Invitrogen), this method was used to transform yeast cells with the recombinant plasmids. To enrich for clones expressing high levels of the Cys-rhEPOs and potentially

containing more than one copy of the integrated vector, transformants were cultivated in media containing a high concentration of Zeocin (2 mg/ml) [23]. Zeocin-resistant transformants were selected, cultured and induced for small-scale expression studies.

#### 3.2. Secreted expression of rhEPO cysteine analogs in *P. pastoris*

To optimize the expression levels of Cys-rhEPOs in *P. pastoris* flask cultures, two important parameters were considered: the pH/buffering conditions and a methanol post-induction regime. Our previous findings indicated that the expression level of PPEPO at a stable pH  $6 \pm 0.5$  was significantly improved compared with that obtained at the other experimentally tested pH values (e.g., a pH range of 4–8) [24]. Accordingly, we used the same pH/buffering conditions to express Cys-rhEPOs. In addition, we found that supplementing the media with 1% (v/v) methanol every 24 h was a more efficient post-induction regime than supplementing with 0.5% (v/v) or 2% (v/v) methanol every 24 h (data not shown). Although it has been shown that methanol concentrations higher than 0.5% (v/v) can potentially lead to toxic effects inside the cell [25], our results are in agreement with other reports indicating that successful post-induction can be achieved in Mut<sup>+</sup> strains using higher concentrations of methanol [26]. Under the conditions defined in the Material and Methods section, expression levels of 100–170 mg/l were obtained for Cys-rhEPOs. The expression levels could possibly be enhanced using a bioreactor in which many important parameters, such as methanol, pH and oxygen levels, can be tightly controlled. Recently, Celik et al. [27] reported an expression level of 130 mg/l for rhEPO in *P. pastoris* using a pilot-scale bioreactor in the presence of the co-substrate sorbitol. The comparable expression levels of Cys-rhEPOs in our flask cultures, when compared with that reported by Celik et al. [27] in the bioreactor, may be attributed to different competencies of the yeast strains. Our results are consistent with other reports [28] that emphasize the importance of screening and using highly expressing clones (ideally harboring multi-copies of the integrated plasmid) to increase the level of recombinant protein expression.

#### 3.3. Characterization of secreted proteins

SDS–PAGE and Western blot analyses of the culture supernatants (Fig. 2) show an intense band of approximately 33 kDa and a faint band at 66 kDa, corresponding to monomeric and dimeric *Pichia*-expressed Cys-rhEPO, respectively. Previously, MALDI–TOF and SDS–PAGE analyses by Celik et al. [6] indicated an average

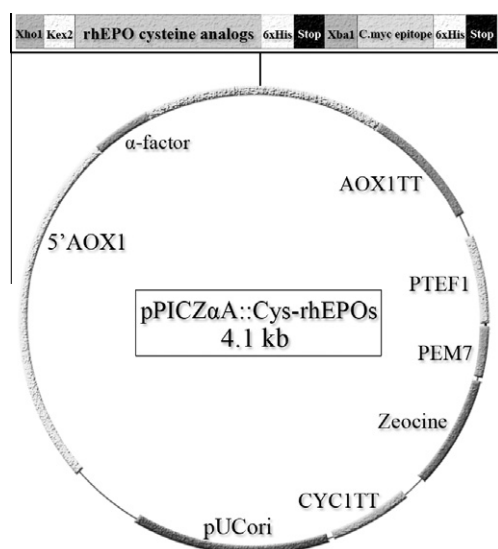


**Fig. 1.** Schematic representation of expression vectors constructed for the Cys-rhEPO analogs. *Xho*I and *Xba*I denote the restriction sites employed for directional cloning of Cys-rhEPO genes into the pPICZ $\alpha$ A vector under control of the *AOX1* promoter and downstream of the secretion ( $\alpha$ -factor) and cleavage (Kex2) sequences. *AOX1* TT, 6xHis, and Stop denote the transcription termination sequence, His tag, and two stop codons (TGA and TAA), respectively.

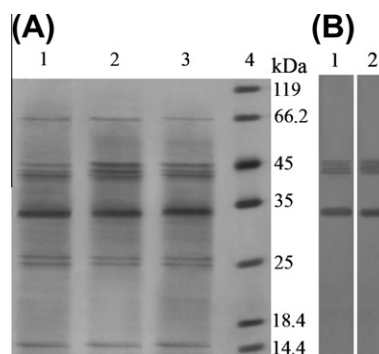


**Fig. 2.** Protein profiles of secreted-EPO analogs 72 h post-induction. (A) For each crude sample, 20  $\mu$ l of supernatant was loaded onto a 5% SDS–PAGE and visualized by silver staining. Lane 1: A1CEPO; Lane 2: E89CEPO; Lane 3: R162CEPO; Lane 4: Protein size marker SM0431 (Fermentas). (B) Western blot analysis of crude E89CEPO was performed using monoclonal anti-human EPO antibody (Lane 1) and monoclonal anti-His (C-term) antibody (Lane 2).



MW of 30–32 kDa for *Pichia*-expressed rhEPO. As shown in Fig. 2, other protein bands are visible in the 42–45 kDa range that interacted with both anti-His and anti-EPO antibodies. N-terminal amino acid analysis of PPEPO [7] demonstrates that the correct processing and complete removal of the  $\alpha$ -factor sequence results in a 33 kDa protein. Therefore, these heavier protein bands may represent an uncleaved form of  $\alpha$ -factor/Cys-rhEPO that was secreted into the culture media as a fusion protein. The secretion of proteins fused to the  $\alpha$ -factor has been reported previously [29] and may be a result of insufficient Kex2 endoprotease processing and removal of the  $\alpha$ -factor secretory signal from the polypeptide chain.

During the purification steps, major parts of the 42–45 kDa proteins could not be removed by IMAC, presumably due to the presence of the C-6xHis-tag in these protein complexes that resulted in their co-purification with correctly processed Cys-rhEPO molecules (data not shown). These protein complexes were removed during the last step of the purification process, as demonstrated for two representative samples of purified Cys-rhEPOs (Fig. 3, lanes 1 and 2).

### 3.4. Bioinformatics analyses

Based on a comprehensive literature review, residues in non-functional regions of rhEPO were considered as candidates for replacement with cysteine. Three-dimensional structures of selected Cys-rhEPOs were generated using homology modeling and were refined and validated by 5–15 ns MD simulations with explicit waters; cysteine-SAA was determined for analogs that were stable during the MD run. Finally, based on the minimum RMSD from native EPO and exhibiting a cysteine-SAA of about half to fully exposed (45–99%) in the final average structure, three Cys-rhEPOs (A1CEPO, E89CEPO, and R162CEPO) were selected for further experimental analysis (Table 1). A representative Ramachandran plot and DOPE score profile, used for the verification of the modeled 3D structure of R162CEPO, are shown in Fig. 4. More than 98% of residues were in the allowed regions of the Ramachandran plot (Table 1). The conformations of the inserted cysteine in the final average structure of three selected Cys-rhEPOs after MD simulation are shown in Fig. 5.

With respect to the importance of free thiol accessibility for successful nucleophilic attack, the cysteine-SAA was quantified in modeled Cys-rhEPOs (Table 1), and three stable analogs with diverse cysteine-SAAs were expressed in *P. pastoris*. The Cys-rhEPO analogs were PEGylated under the same conditions to compare the

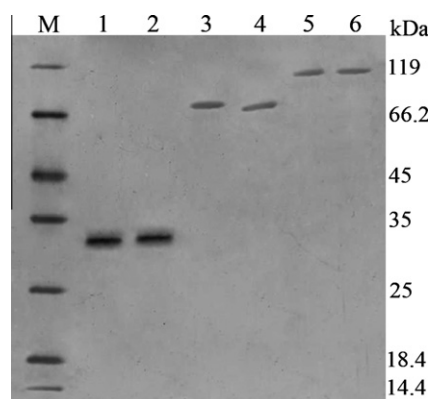


**Fig. 3.** Silver-stained SDS-PAGE analysis of representative purified EPO cysteine analogs and their PEGylated conjugates. Lane M: Protein size marker SM0431 (Fermentas); Lane 1: E89CEPO; Lane 2: R162CEPO; Lane 3: 20 kDa PEG-E89CEPO; Lane 4: 20 kDa PEG-R162CEPO; Lane 5: 30 kDa PEG-E89CEPO; Lane 6: 30 kDa PEG-R162CEPO.

**Table 1**

Comparison of structural properties among the modeled Cys-rhEPOs.

Cys-rhEPOs	All-atom RMSD <sup>a</sup> (in.)	Ramachandran <sup>b</sup>	SAA (%) <sup>c</sup>
A1CEPO	2.991	98.6 (93.2)	48.8
E89CEPO	2.706	98.4 (91.2)	96.6
R162CEPO	3.127	98.5 (92.5)	72.9

<sup>a</sup> All-atom root mean square deviation (RMSD) of modeled analog from native EPO in Å.

<sup>b</sup> Percentage of residues in the 'allowed' and 'most favored' (between brackets) regions of the Ramachandran plot.

<sup>c</sup> Surface area accessibility (SAA) of engineered cysteine residues in the modeled Cys-rhEPOs.

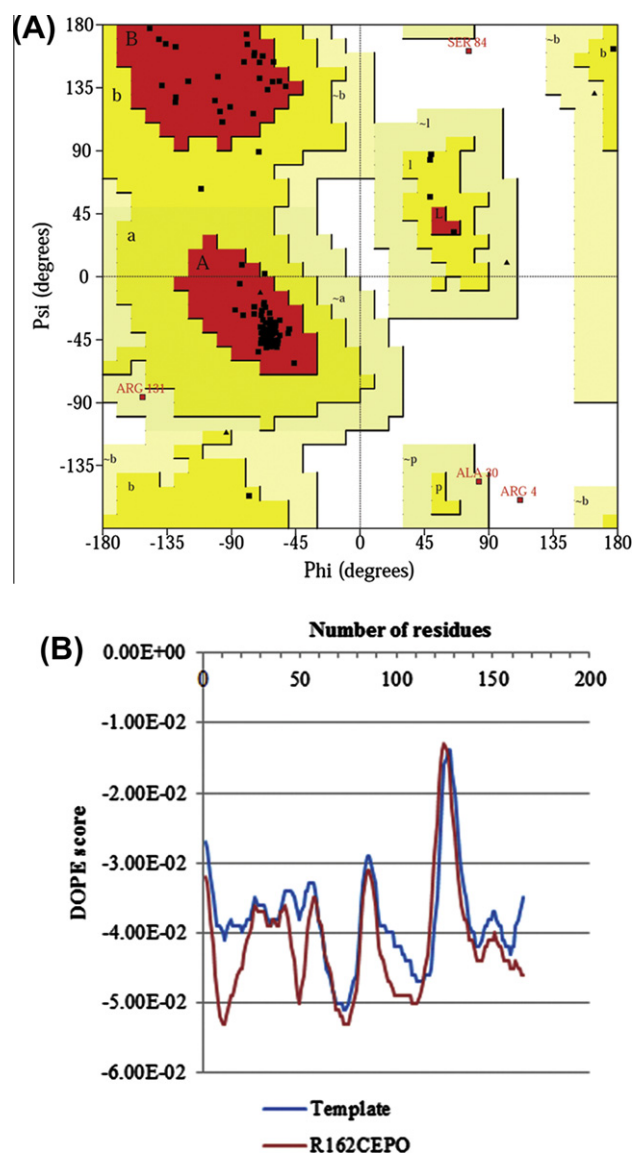


**Fig. 4.** An example of the quality assessment of the modeled 3D structure of R162CEPO. (A) Ramachandran plot and (B) DOPE score profile.

yields of produced PEG-Cys-rhEPO conjugates with the corresponding cysteine-SAA of their parent molecules.

### 3.5. Preparation of PEGylated EPO cysteine analogs

The Cys-rhEPOs and PPEPO were incubated with 20 kDa and/or 30 kDa mPEG-maleimide in the presence of TCEP reducing agent.

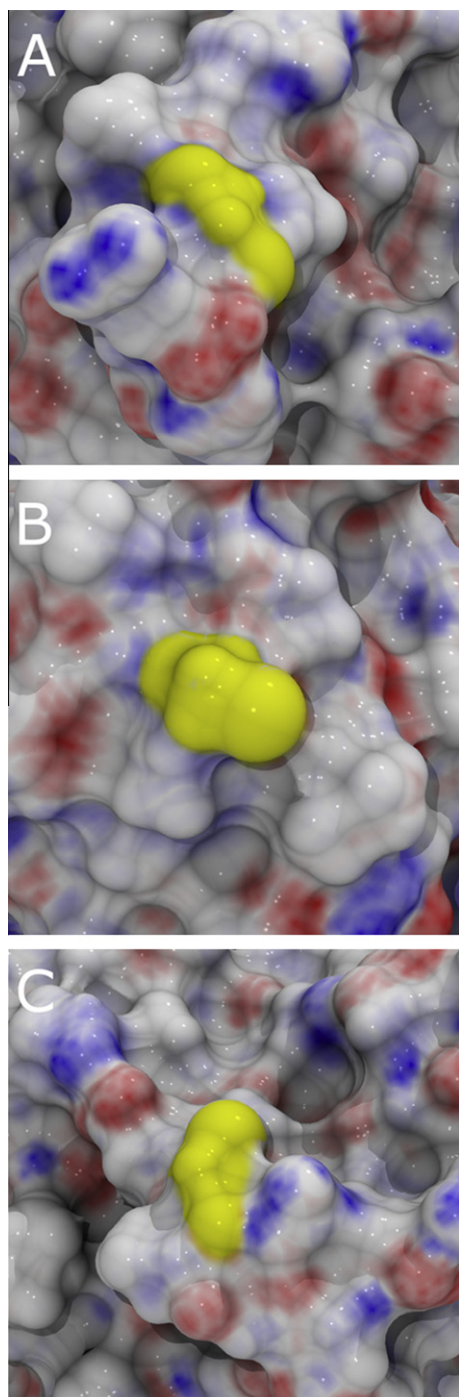


**Fig. 5.** The conformation of the inserted cysteine in the final average structure of three selected Cys-rhEPOs after MD simulation with different surface area accessibility of engineered cysteine residues (cysteine-SAA). The engineered cysteine residues are colored in yellow. (A) A1CEPO with cysteine-SAA of 48.8%, (B) E89CEPO with cysteine-SAA of 96.6%, and (C) R162CEPO with cysteine-SAA of 72.9%.

Prior to harvesting of Cys-rhEPOs, 2 mM cysteine was added to the supernatants of the corresponding cultures to stabilize the molecule through the formation of a temporary disulfide bond with the free cysteine residue. Partial reduction using TCEP breaks these artificially formed disulfide bridges and makes the extra cysteine residue free and accessible to react with the PEGylating agent [30]. Due to the high water solubility of TCEP, this reducing agent is generally impermeable to the hydrophobic protein core,

allowing for its use in the selective reduction of disulfide bonds that are exposed to the aqueous environment [31]. Accordingly, it seems likely that the native disulfide bridges in Cys-rhEPOs remained intact under these reducing conditions in the PEGylation reactions because, while Cys-rhEPOs could effectively react with mPEG-maleimide, PPEPO did not react with this PEGylating agent.

Under the conditions described, we obtained only mono-PEGylated Cys-rhEPOs with approximate yields that are represented in Table 2. The yields of PEG-Cys-rhEPO conjugates were directly related to the corresponding cysteine-SAA of their parent molecules (Table 1) and conversely were affected by their PEG size. Therefore, among the PEG-Cys-rhEPO conjugates produced, the PEG-E89CEPO conjugates with the highest (96.6%) cysteine-SAA showed the largest yields. In addition, our results indicate that because there was no significant difference in the yields of the 20 kDa and 30 kDa PEGylated E89CEPOs (Table 2), the high surface accessibility of the free cysteine residue may balance the hindering effect of larger polymers. Low cysteine-SAA can amplify the steric hindrance of high molecular weight polymers for functional groups and may lead to the production of low ratios of the conjugates. To overcome the steric hindrance of bulky biomolecules and polymers that are involved in bioconjugation reactions, other approaches such as the incorporation of a spacer molecule or adjusting the reaction conditions to increase the reactivity of the coupling agents may also be considered [32]. Further studies are needed to elucidate the impact of surface accessibility and steric hindrance on the efficiency of protein-PEG conjugation.

Silver-stained SDS-PAGE analysis of representative purified PEG-Cys-rhEPO conjugates is shown in Fig. 3 (lanes 3–6) and demonstrates that the conjugates were successfully separated from unreacted EPO and PEG molecules by the purification strategy employed. The final purities of Cys-rhEPOs and their PEG conjugates at the end of two purification steps were more than 98% as determined by SE-HPLC (data not shown).

### 3.6. In vitro bioassay

The in vitro bioactivities of rhEPO, *Pichia*-expressed EPO analogs, and PEG-Cys-rhEPO conjugates were assessed by measuring their ability to support the proliferation of UT-7 cell lines. The bioassay results are summarized in Table 3. The Cys-rhEPOs had EC50 values (the protein concentration needed for 50% of the maximum proliferative effect) that were almost equivalent to that of PPEPO. Moreover, as shown in Table 3, the EC50 values for *Pichia*-expressed EPO proteins were approximately 30% less than that of CHO cell-expressed rhEPO. Apparently, replacing a single amino acid with a cysteine in selected positions and the presence of a C-6xHis-tag did not adversely affect the in vitro activities of the Cys-rhEPOs. The increase in in vitro bioactivity observed for *Pichia*-expressed EPO proteins may be the result of the attachment of non-sialylated simple sugars [predominantly Man<sub>17</sub>(GlcNAc)<sub>2</sub> for N-linked glycosylation sites] [6] to the polypeptide backbone. It has been recognized that sugars are not essential for the in vitro activity of EPO, and removal of the terminal sialic acid

**Table 2**

The approximate yields of produced PEG-Cys-rhEPO conjugates.

PEG-Cys-rhEPO conjugates	Yields (%)
20 kDa PEG-A1CEPO	45
30 kDa PEG-A1CEPO	30
20 kDa PEG-E89CEPO	85
30 kDa PEG-E89CEPO	80
20 kDa PEG-R162CEPO	65
30 kDa PEG-R162CEPO	55

**Table 3**

The in vitro bioassay results for EPO proteins and PEG-Cys-rhEPO conjugates.

Proteins	EC50 values <sup>a</sup> of non-PEGylated EPO proteins	EC50 values of 20 kDa PEGylated Cys-rhEPOs	EC50 values of 30 kDa PEGylated Cys-rhEPOs
rhEPO <sup>b</sup>	0.41 ± 0.11		
PPEPO <sup>c</sup>	0.30 ± 0.07		
A1CEPO	0.25 ± 0.05	0.38 ± 0.09	0.77 ± 0.16
E89CEPO	0.31 ± 0.08	0.32 ± 0.07	0.48 ± 0.12
R162CEPO	0.27 ± 0.06	0.39 ± 0.11	0.73 ± 0.14

Data are means ± SD (n = 3).

<sup>a</sup> EC50 (ng/ml): protein concentration that stimulates 50% of maximal stimulation.<sup>b</sup> CHO-derived rhEPO (R&D Systems, Inc.).<sup>c</sup> *Pichia*-expressed rhEPO [7].

residues may increase the in vitro efficacy of EPO due to its enhanced affinity for the receptor [33]. Although attachment of the highly flexible long PEG chain to proteins could lead to masking of receptor binding sites in the same way, this drawback may be minimized by targeted-PEGylation strategies [12]. In this context, compared with unmodified Cys-rhEPOs, PEG-Cys-rhEPO conjugates showed a loss of in vitro activity that was directly related to their PEG size (Table 3). However, the in vitro activities of 30-kDa PEG-Cys-rhEPO conjugates were comparable to that of 20 kDa mono-N-terminal PEG-PPEPO with a mean EC50 of 0.52 ng/ml [7]. In contrast to the cysteine-specific PEGylation approach, 'complete' selectivity could not be achieved through the reductive alkylation of proteins with PEG-aldehydes [34], and this issue may give rise to a slight modification of amino groups on lysine residues that are involved in protein–receptor interactions [35]. In addition, the 30 kDa PEG conjugates of A1CEPO and R162CEPO showed greater losses in bioactivities compared with the 30 kDa PEG-E89CEPO. Although the three replaced amino acid residues are not close to the receptor binding sites of the protein [36], the steric hindrance effect of the PEG chain on ligand–receptor interactions appears to be minimal for PEG-E89CEPO. Nevertheless, all of the PEGylated *Pichia*-expressed EPO analogs were biologically active and had EC50 values that were comparable to that of rhEPO. In agreement with our results, Long et al. [30] reported that PEGylated insect cell-expressed EPO cysteine analogs retained in vitro bioactivity.

### 3.7. Pharmacokinetic studies in rabbits

Serum levels of rhEPO, E89CEPO, and its 20 kDa and 30 kDa PEGylated conjugates were determined for up to 72 h following

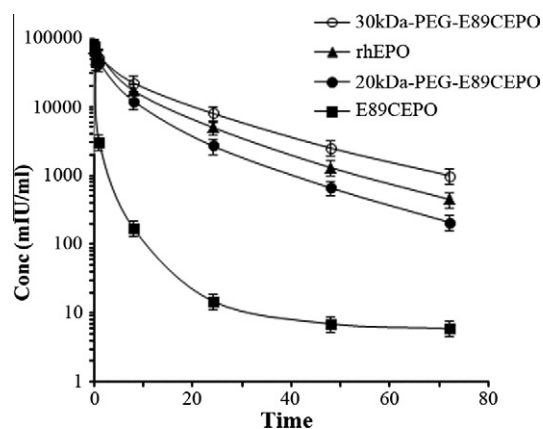


**Fig. 6.** Mean serum concentration vs. time profiles of rhEPO (R&D Systems), E89CEPO, 20 kDa and 30 kDa PEG-E89CEPO in normal rabbits. Animals received a single intravenous injection of samples, each at a dose of 15 µg protein/kg. Protein levels were measured using human EPO ELISA kits. Data are means ± SD for 3 rabbits per group.

their intravenous administration to rabbits. The plasma level–time curves of the samples declined biexponentially and were fitted to a two-compartmental model (Fig. 6). Each rabbit received 15 µg (2700 IU) of protein/kg body weight, and an activity of 180 IU/µg was assumed for the EPO proteins. The pharmacokinetic parameters are summarized in Table 4. The central volumes of distribution [ $V_c = \text{Dose}/C_p(0)$ ] for PEG-E89CEPO conjugates were comparable to those for rhEPO and E89CEPO and were close to the plasma volume of a rabbit, which points to a limited extravascular transport during the initial distribution phase. The increased steady state volume of distribution ( $V_{ss}$ ) relative to estimated  $V_c$  values for all of the samples (especially E89CEPO) indicates a subsequent capillary transport of samples out of the vascular system and/or their binding to EPO receptors (EPO-Rs) on vascular endothelial cells. However, the significantly (30–50%) lower  $V_{ss}$  values of the PEG-E89CEPO conjugates compared with that of E89CEPO suggest that the PEG conjugation of E89CEPO resulted in a slower extravascular distribution and/or lower binding of the conjugates to EPO-Rs expressed on non-hematopoietic endothelial cells. Our finding that the  $V_c$  and  $V_{ss}$  values of PEGylated EPO conjugates were comparable to those of rhEPO is in agreement with findings from other studies [1,37]. Once the drug distribution has been established, changes in plasma levels are mainly reflected by drug elimination parameters. The estimated clearance rates of 20 kDa and 30 kDa PEG-E89CEPOs were 18- and 56-fold slower, respectively, than that of E89CEPO (Table 4). The terminal half-lives [ $t_{1/2}(\beta)$ ] of the PEG-E89CEPO conjugates were 4–5-fold longer than the  $t_{1/2}(\beta)$  of the E89CEPO. Moreover, for PEGylated E89CEPO molecules, the mean residence times (MRT) increased 7–12-fold compared with that of the unmodified E89CEPO. The MRT of the 20 kDa PEG-E89CEPO was similar to the MRT of 20 kDa N-terminal PEG-PPEPO ( $9.7 \pm 0.4$  h) [7] and was comparable with that of rhEPO (Table 4). However, the 30 kDa PEG-E89CEPO demonstrated a significant (approximately 30%) increase in the mean residence time compared with rhEPO. Substantial changes in  $CL$ ,  $t_{1/2}(\beta)$  and MRT, but not in  $V_c$  and  $V_{ss}$ , suggest that the PEGylation mostly affected the elimination phase of EPO pharmacokinetic profile. Therefore, regardless of the mechanism, the large reduction in the systemic clearance can be considered as the main reason for the extended plasma residency and longer half-life of the PEG-E89CEPO conjugates relative to those of E89CEPO.

### 3.8. Erythropoietic activity assay

RhEPO, E89CEPO, and its PEGylated conjugates were evaluated using the normocythemic mouse assay to compare their erythropoietic activities in terms of reticulocyte percentage (RET%) in the blood samples. The changes in RET% were determined microfluorometrically following subcutaneous administration of each sample and throughout a 14-day period. While no in vivo efficacy could be determined for E89CEPO under the test conditions, the

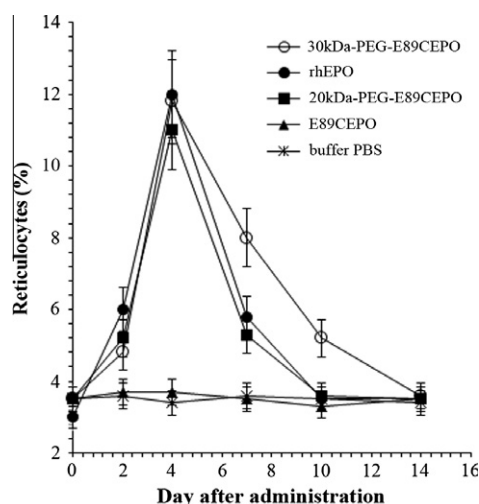


**Table 4**

Summary of pharmacokinetic parameters of rhEPO, E89CEPO, and PEG–E89CEPO conjugates following intravenous administration in rabbits.

Pharmacokinetic parameters	rhEPO <sup>a</sup>	E89CEPO	20 kDa PEG–E89CEPO	30 kDa PEG–E89CEPO
Terminal half-life (h)	13.3 ± 1.6	3.1 ± 0.3	13.1 ± 1.4	16.1 ± 2.1
V <sub>c</sub> (ml/kg) <sup>b</sup>	38.3 ± 5.5	36.1 ± 5.3	41.9 ± 7.8	42.3 ± 8.1
V <sub>ss</sub> (ml/kg) <sup>c</sup>	75.8 ± 9.2	173.0 ± 22.2	115.3 ± 13.1	79.8 ± 10.7
Clearance (ml/h/kg)	8.2 ± 1.1	277.6 ± 29.2	15.4 ± 1.7	5.3 ± 0.7
[AUC] <sub>0–∞</sub> (mlU h/ml) <sup>d</sup>	601541 ± 59100	35111 ± 3720	416987 ± 57500	747463 ± 82300
MRT (h) <sup>e</sup>	11.1 ± 1.3	1.3 ± 0.2	9.3 ± 1.0	16.1 ± 1.9

Results are means ± SD for three rabbits per group.

<sup>a</sup> CHO-derived rhEPO (R&D Systems, Inc.).<sup>b</sup> Central volume of distribution [V<sub>c</sub> = Dose/Cp(0)].<sup>c</sup> Steady state volume of distribution.<sup>d</sup> Area under the concentration vs. time curve (extrapolated to infinity).<sup>e</sup> Mean residence time.**Fig. 7.** Evaluations of in vivo activities of E89CEPO, 20 kDa and 30 kDa PEGylated E89CEPOs and rhEPO (R&D Systems) using the normocythemmic mice assay. Reticulocyte percentages were determined microfluorometrically following subcutaneous administration of each sample at a dose of 10 µg/kg body weight. Data are means ± SD for six mice per group.

20 kDa PEG–E89CEPO demonstrated an activity that was comparable to that of rhEPO (Fig. 7). Moreover, our results demonstrated a longer erythropoietic activity for the 30 kDa PEG–E89CEPO compared with that of rhEPO. When the RET% of the rhEPO remained higher than baseline for 7 days, the 30 kDa PEG–E89CEPO maintained an RET% above baseline for 11–12 days.

EPO exerts its erythropoietic action through binding to specific cell-surface receptors (hematopoietic EPO-Rs), which are abundantly expressed on erythroid progenitor cells that are located mainly in the bone marrow [38]. Non-hematopoietic EPO-Rs with different biological effects have also been identified on myocytes, neuronal cells, and endothelial cells [39]. The binding activity and circulating longevity are the key factors that dominate the bio-activity of ESAs in vivo [37]. Therefore, considering the in vitro activities of PEG–Cys-rhEPO conjugates, which reflect the corresponding preservation of their ability to bind EPO-Rs, the increased and prolonged in vivo potencies of PEGylated EPO analogs are attributable to their substantially reduced systemic clearance rates and longer plasma residencies relative to those of their unmodified parent molecules.

The mechanism(s) by which PEGylation affects the clearance pathways of EPO have not been fully elucidated mainly because the mechanism(s) of rhEPO clearance, and the site(s) of its degradation have not been definitively characterized [1]. Multiple mechanisms and pathways have been suggested for the clearance

of EPO and EPO analogs in the body. Although initial experiments suggested that rhEPO elimination was predominantly achieved through renal and hepatic excretion pathways, subsequent investigations determined that the liver and kidney do not play a major role in the clearance of sialylated rhEPO [40]. However, it has been shown that the desialylated and/or non-sialylated EPO molecules are rapidly eliminated by hepatic asialoglycoprotein receptors, which, in case of *Pichia*-expressed EPOs, suggests that mannose/ N-acetyl glucosamine receptors may be primarily involved [41]. Therefore, the restored in vivo activities of PEGylated *Pichia*-expressed EPO conjugates can be attributed to the shielding effect and steric hindrance of polymeric chains surrounding the protein and to preventing its interaction with the asialoglycoprotein receptors. The recovery of in vivo potency of non-sialylated EPO using the PEGylation technique has already been reported [3,7,13].

The prolonged erythropoietic activity of the 30 kDa PEG–E89CEPO relative to that of rhEPO suggests that PEGylation may possibly impact the clearance of E89CEPO by more than one mechanism. Recent evidence strongly suggests that an important pathway for the clearance of ESAs is through the binding of ligands to surface hematopoietic and/or non-hematopoietic EPO-Rs, followed by internalization of the ligand–receptor complex and degradation in lysosomes [42]. It has been shown that PEGylation or hyperglycosylation of ESAs can result in reduced ligand binding affinity for EPO-Rs [43]. Therefore, the reduced clearance of PEGylated ESAs may be partially ascribed to their impact on EPO-Rs-mediated clearance pathways [42]. It is possible that there are other eliminating processes (EPO-Rs independent pathways) for ESAs that could also be impacted by PEGylation [37]. The protective effect of the PEG shell surrounding the protein can reduce immunogenic recognition, increase resistance to degradation by proteolytic enzymes [12], and enhance physicochemical stability. Moreover, the increased hydrodynamic size of PEGylated ESAs (due to the attached hydrated PEG strands) could result in a decrease in their capillary transport from the blood to eliminating organs, such as the kidney, interstitial fluid, and the lymphatic system [44]. Further investigations are necessary to determine the individual contributions of the multiple mechanisms that have been proposed for the clearance of EPO and its long-lasting analogs. Our results are consistent with a number of previous studies which showed that a reduction in the clearance of rhEPO or its analogs (by PEGylation or other strategies such as hyperglycosylation) results in an increased and prolonged in vivo erythropoietic activity, which may allow for extending the intervals between doses of the drug [10,37,45]. However, Wang et al. [46] reported that despite the substantial (approximately 50%) lower clearance of 40 kDa PEGylated *E. coli*-expressed EPO compared with that of rhEPO, no significant difference was observed in their in vivo activities. This discrepancy may be attributed to the low stability of non-glycosylated *E. coli*-expressed EPO [3,46,47] which



could lead to conformational changes and losses in EPO-Rs binding activity that are required for erythropoiesis-stimulating effects. These results demonstrate the significant role native glycosylation plays in the physicochemical and conformational stability of EPO.

In summary, the present study demonstrates the feasibility of using *P. pastoris* as a well-defined expression system for the cost-effective production of rhEPO and its engineered cysteine analogs that exhibit increased in vitro activity and a preserved physicochemical stability. Moreover, we demonstrate that the in vivo serum residency and erythropoietic activity of non-sialylated *Pichia*-expressed EPO can be substantially increased and prolonged through site-directed PEGylation approaches. In addition, this approach may allow for a less frequent administration regimen for the protein compared with rhEPO. Future studies will be directed toward achieving tightly controlled expression of EPO and its analogs using bioreactors to obtain higher expression levels and to optimize PEG coupling conditions to further improve the efficiency of conjugation. Targeted PEGylation of *Pichia*-expressed proteins/peptides can be regarded as a versatile and productive strategy for generating low-cost and long-acting therapeutic proteins.

## References

- [1] S. Elliott, E. Pham, I.C. Macdougall, Erythropoietins: a common mechanism of action, *Exp. Hematol.* 36 (2008) 1573–1584.
- [2] J. Egrie, The cloning and production of recombinant human erythropoietin, *Pharmacotherapy* 10 (1990) 3S–8S.
- [3] Y.J. Wang, Y.D. Liu, J. Chen, et al., Efficient preparation and PEGylation of recombinant human non-glycosylated erythropoietin expressed as inclusion body in *E. Coli*, *Int. J. Pharm.* 386 (2010) 156–164.
- [4] M. Nagao, K. Inoue, S.K. Moon, S. Masuda, et al., Secretory production of erythropoietin and the extracellular domain of the erythropoietin receptor by *Bacillus brevis*: affinity purification and characterization, *Biosci. Biotechnol. Biochem.* 61 (1997) 670–674.
- [5] S. Elliott, J. Giffin, S. Suggs, E.P. Lau, A.R. Banks, Secretion of glycosylated human erythropoietin from yeast directed by the alpha-factor leader region, *Gene* 79 (1989) 167–180.
- [6] E. Celik, P. Calik, S.M. Halloran, S.G. Oliver, Production of recombinant human erythropoietin from *Pichia pastoris* and its structural analysis, *J. Appl. Microbiol.* 103 (2007) 2084–2094.
- [7] A. Maleki, A.R. Najafabadi, F. Roohvand, A. Shafiee, H. Faghihi, M.H. Hedayati, H. Tajerzadeh, Evaluation of bioactivity pharmacokinetic characteristics of PEGylated *P. pastoris*-expressed erythropoietin analogs, *Drug. Deliv.* 18 (2011) 570–577.
- [8] M. Bollok, D. Resina, F. Valero, P. Ferrer, Recent patents on the *Pichia pastoris* expression system: expanding the toolbox for recombinant protein production, *Recent. Pat. Biotechnol.* 3 (2009) 192–201.
- [9] G.P.L. Cereghino, J.M. Cregg, Heterologous protein expression in the methylotrophic yeast *Pichia pastoris*, *FEMS Microbiol. Rev.* 24 (2000) 45–66.
- [10] J.C. Egrie, E. Dwyer, J.K. Browne, A. Hitz, M.A. Lykos, Darbepoetin alfa has a longer circulating half-life and greater in vivo potency than recombinant human erythropoietin, *Exp. Hematol.* 31 (2003) 290–299.
- [11] S.R. Hamilton, R.C. Davidson, N. Sethuraman, J.H. Nett, et al., Humanization of yeast to produce complex terminally sialylated glycoproteins, *Science* 313 (2006) 1441–1443.
- [12] J.M. Harris, N.E. Martin, M. Modi, PEGylation: a novel process for modifying pharmacokinetics, *Clin. Pharmacokinet.* 40 (2001) 539–551.
- [13] K.D. Yesland, Pharmacodynamically Enhanced Therapeutic Proteins, US Patent 2008/0171696, 2008.
- [14] R.J. Goodson, N.V. Katre, Site-directed PEGylation of recombinant interleukin-2 at its glycosylation site, *Biotechnology* 8 (1990) 343–346.
- [15] R.M. Horton, *In vitro* recombination and mutagenesis of DNA. SOIn together tailor-made genes, in: B.A. White (Ed.), *Methods in Molecular Biology*, Vol. 15: PCR Protocols: Current Methods and Applications, Humana Press, Totawa, NJ, 1993, pp. 251–266.
- [16] T. Mosmann, Rapid colorimetric assay for cellular growth and survival: application to proliferation and cytotoxicity assays, *J. Immunol. Methods* 65 (1983) 55–63.
- [17] A. Sali, T.L. Blundell, Comparative protein modelling by satisfaction of spatial restraints, *J. Mol. Biol.* 234 (1993) 779–815.
- [18] D. Van der Spoel, E. Lindahl, B. Hess, G. Groenhof, A.E. Mark, H.J. Berendsen, GROMACS: fast, flexible, and free, *J. Comput. Chem.* 26 (2005) 1701–1718.
- [19] J.D. Gans, D. Shalloway, Qmol: a program for molecular visualization on Windows-based PCs, *J. Mol. Graph. Model.* 19 (2001) 557–559.
- [20] R. Fraczekiewicz, W. Braun, Exact and efficient analytical calculation of the accessible surface areas and their gradients for macromolecules, *J. Comput. Chem.* 19 (1998) 319–333.
- [21] M.M. Bradford, A rapid and sensitive for the quantitation of microgram quantities of protein utilizing the principle of protein dye binding, *Anal. Biochem.* 72 (1976) 248–254.
- [22] U.K. Laemmli, Cleavage of structural proteins during assembly of head of bacteriophage-T4, *Nature* 227 (1970) 680–685.
- [23] A.J. Sunga, I. Tolstorukov, J.M. Cregg, Post-transformational vector amplification in the yeast *Pichia pastoris*, *FEMS. Yeast. Res.* 8 (2008) 870–876.
- [24] A. Maleki, F. Roohvand, H. Tajerzadeh, H. Khanahmad, M.B. Nobari, A. Beiruti, A.R. Najafabadi, High expression of methylotrophic yeast-derived recombinant human erythropoietin in a pH-controlled batch system, *Avicenna. J. Med. Biotech.* 2 (2010) 197–206.
- [25] W. Zhang, M.A. Bevins, B.A. Plantz, L.A. Smith, M.M. Meagher, Modeling *Pichia pastoris* growth on methanol and optimizing the production of a recombinant protein, the heavy-chain fragment C of botulinum, serotype A, *Biotechnol. Bioeng.* 70 (2000) 1–8.
- [26] D.W. Murray, S.J.B. Duff, P.H. Lanthier, Induction and stability of alcohol oxidase in the methylotrophic yeast *Pichia pastoris*, *Appl. Microbiol. Biotechnol.* 32 (1989) 95–100.
- [27] E. Celik, P. Calik, S.G. Oliver, Fed-batch methanol feeding strategy for recombinant protein production by *Pichia pastoris* in the presence of co-substrate sorbitol, *Yeast* 26 (2009) 473–484.
- [28] J.J. Clare, M.A. Romanos, F.B. Rayment, J.E. Rowedder, M.A. Smith, et al., Production of epidermal growth factor in yeast: High-level secretion using *Pichia pastoris* strains containing multiple gene copies, *Gene* 105 (1991) 205–212.
- [29] K.M. Zsebo, H-S. Lu, J.C. Fieschko, et al., Protein secretion from *Saccharomyces cerevisiae* directed by the prepro- $\alpha$ -factor leader region, *J. Biol. Chem.* 261 (1986) 5858–5865.
- [30] D.L. Long, D.H. Doherty, S.P. Eisenberg, et al., Mono-pegylated erythropoietin analogs with preserved in vitro bioactivity, *Exp. Hematol.* 34 (2006) 697–704.
- [31] E.B. Getz, M. Xiao, T. Chakrabarty, R. Cooke, P.R. Selvin, A comparison between the sulfhydryl reductants tris(2-carboxyethyl)phosphine and dithiothreitol for use in protein biochemistry, *Anal. Biochem.* 273 (1999) 73–80.
- [32] J. Khandare, T. Minko, Polymer–drug conjugates: progress in polymeric prodrugs, *Prog. Polym. Sci.* 31 (2006) 359–397.
- [33] E. Tsuda, G. Kawanishi, M. Ueda, S. Masuda, R. Sasaki, The role of carbohydrate in recombinant human erythropoietin, *Eur. J. Biochem.* 188 (1990) 405–411.
- [34] O.B. Kinstler, N.E. Gabriel, C.E. Farrar, R.B. DePrince, N-Terminally Chemically Modified Protein Compositions and Method, US Patent 5985265, 1999.
- [35] D.M. Wojchowski, L. Caslake, Biotinylated recombinant human erythropoietins: bioactivity and utility as receptor ligand, *Blood* 74 (1989) 952–958.
- [36] J.P. Boissel, W.R. Lee, S.R. Presnell, F.E. Cohen, H.F. Bunn, Erythropoietin structure–function relationships. Mutant proteins that test a model of tertiary structure, *J. Biol. Chem.* 268 (1993) 15983–15993.
- [37] B. Agoram, K. Aoki, S. Doshi, C. Gegg, G. Jang, G. Molineux, L. Narhi, S. Elliott, Investigation of the effects of altered receptor binding activity on the clearance of erythropoiesis-stimulating proteins: nonerythropoietin receptor-mediated pathways may play a major role, *J. Pharm. Sci.* 98 (2008) 2198–2211.
- [38] V.C. Broudy, N. Lin, M. Brice, B. Nakamoto, T. Papayannopoulou, Erythropoietin receptor characteristics on primary human erythroid cells, *Blood* 77 (1991) 2583–2590.
- [39] S.E. Juul, A.T. Yachnis, R.D. Christensen, Tissue distribution of erythropoietin erythropoietin receptor in the developing human fetus, *Early. Human. Dev.* 52 (1998) 235–249.
- [40] J.A. Widness, P. Veng-Pedersen, R.L. Schmidt, L.S. Lowe, J.A. Kisthard, C. Peters, *In vivo* <sup>125</sup>I-erythropoietin pharmacokinetics are unchanged after anesthesia, nephrectomy and hepatectomy in sheep, *J. Pharmacol. Exp. Ther.* 279 (1996) 1205–1210.
- [41] J.L. Spivak, B.B. Hogans, The in vivo metabolism of recombinant human erythropoietin in the rat, *Blood* 73 (1989) 90–99.
- [42] A.W. Gross, H.F. Lodish, Cellular trafficking and degradation of erythropoietin and novel erythropoiesis stimulating protein (NESP), *J. Biol. Chem.* 281 (2006) 2024–2032.
- [43] M. Jarsch, M. Brandt, M. Lanzendorfer, A. Haselbeck, Comparative erythropoietin receptor binding kinetics of CERA and epoetinbeta determined by surface plasmon resonance and competition binding assay, *Pharmacology* 81 (2007) 63–69.
- [44] T. Yamaoka, Y. Tabata, Y. Ikada, Distribution and tissue uptake of poly(ethylene glycol) with different molecular weights after intravenous administration to mice, *J. Pharm. Sci.* 83 (1994) 601–606.
- [45] I.C. Macdougall, R. Robson, S. Opatna, X. Liogier, et al., Pharmacokinetics and pharmacodynamics of intravenous and subcutaneous continuous erythropoietin receptor activator (CERA) in patients with chronic kidney disease, *Clin. J. Am. Soc. Nephrol.* 1 (2006) 1211–1215.
- [46] Y-J. Wang, S-J. Hao, Y-D. Liu, T. Hu, et al., PEGylation markedly enhances the in vivo potency of recombinant human non-glycosylated erythropoietin: A comparison with glycosylated erythropoietin, *J. Control. Release* 145 (2010) 306–313.
- [47] L.O. Narhi, T. Arakawa, K.H. Aoki, R. Elmore, M.F. Rohde, T. Boone, T.W. Strickland, The effect of carbohydrate on the structure and stability of erythropoietin, *J. Biol. Chem.* 266 (1991) 23022–23026.